

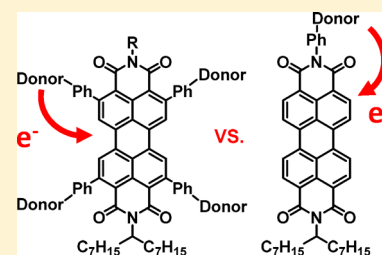
Photoinduced Electron Transfer in 2,5,8,11-Tetrakis-Donor-Substituted Perylene-3,4:9,10-bis(dicarboximides)

Leah E. Shoer, Samuel W. Eaton, Eric A. Margulies, and Michael R. Wasielewski*

Department of Chemistry and Argonne-Northwestern Solar Energy Research (ANSER) Center, Northwestern University, Evanston, Illinois 60208-3113, United States

Supporting Information

ABSTRACT: A series of electron donor–acceptor compounds based on substitution of perylene-3,4:9,10-bis(dicarboximide) (PDI) with four electron donors at the 2,5,8,11-positions were synthesized and characterized using femtosecond transient absorption spectroscopy. The distance between the PDI and the *N,N*-dimethylaniline or phenothiazine donors was varied using one or two phenyl groups. Photoexcitation of PDI results in rapid charge separation followed by charge recombination with time constants ranging from tens of picoseconds to nanoseconds. The electron transfer time constants are compared with those of the corresponding molecules in which the donor is attached to the PDI through its imide nitrogen atom. The electron transfer reactions through the 2,5,8,11-positions of PDI are generally much faster than those through the imide nitrogen positions, in concert with stronger donor electronic coupling to the PDI acceptor core and in contrast to substituents at the imide positions through which the HOMO and LUMO nodal planes pass.



INTRODUCTION

Increasing worldwide energy demand has spurred research on developing and improving renewable energy technology. Materials based on small organic molecules have been successfully applied in organic electronic technologies such as organic field-effect transistors (OFETs) and organic photovoltaics (OPVs),^{1–4} but the resultant devices in the case of OPVs have not yet attained efficiencies or stabilities that make them commercially viable. One concern that greatly impacts the efficiency of such small-molecule devices is intermolecular organization and interaction within the active layer.^{5–7} Small molecules that have suitable photoinitiated charge separation behavior, the ability to self-organize into appropriate geometries, and structures that mitigate unfavorable intermolecular contact may address efficiency loss pathways such as charge trapping.^{8–10}

Perylene-3,4:9,10-bis(dicarboximide) (PDI) is a promising small-molecule building block for use as an electron-accepting chromophore in OPV active layers. PDI has a high extinction coefficient that makes it well-suited for use in light-absorbing applications.^{11,12} It also has favorable redox potentials that make it suitable as an electron acceptor in charge separation systems.^{13,14} Furthermore, because of its flat, aromatic structure, PDI exhibits strong π -stacking behavior in single crystals, thin films, and solution-phase aggregates.^{15–19} Examples of systems that take advantage of one or both of these properties are well-known in the literature.^{20–23} We have demonstrated previously that a PDI acceptor symmetrically substituted with electron donors can undergo two-step charge separation to generate a long-lived radical ion pair (RP).²⁴ Dissolving this donor–acceptor system in methylcyclohexane results in self-assembly into a helical hexamer in which the PDI

molecules are π -stacked. However, as a result of the helical nature of the assembly, the terminal donor groups are too far apart to ensure sufficient electronic coupling for hole hopping or delocalization to occur.

Substitution at the 1,6,7,12-positions (“bay positions”) of PDI introduces varying degrees of PDI core distortion away from planarity, which is frequently reflected in the structures of its self-assembled aggregates as in the system described above. In contrast, substitution at the 2,5,8,11-positions (“headland positions”) does not lead to these distortions.^{25,26} Indeed, structures containing phenyl substituents at the headland positions show good slip-stacked alignment between both adjacent PDI cores and the appended substituents.²⁷ We have recently shown that the slip-stacked alignment of PDI cores significantly improves the performance of OPVs relative to unsubstituted PDI acceptors that stack cofacially, for example, achieving a device power conversion efficiency of 3.7% when blended with the donor polymer PBTI3T.²⁸ This geometrical arrangement should be favorable for OPV active layers for two reasons. First, it is amenable to the formation of segregated charge transport conduits for both holes and electrons, which should facilitate long-range charge hopping, leading to efficient charge extraction at an electrode. Second, the acceptor moiety is insulated from contact with other donor moieties in adjacent molecular stacks, diminishing intermolecular charge recombination (Figure 1). Headland substituents provide an accessible path toward such a supramolecular assembly.

Special Issue: John R. Miller and Marshall D. Newton Festschrift

Received: November 20, 2014

Revised: December 1, 2014

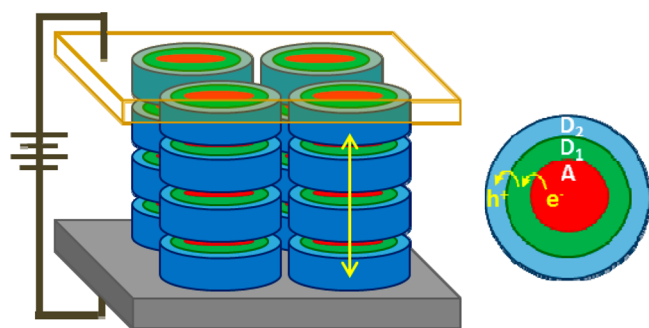


Figure 1. Schematic representation of the ideal architecture for an OPV active layer. In this case, red = acceptor, green = primary donor, blue = secondary donor.

Here we present the synthesis and photophysical characterization of a series of PDI derivatives substituted with aromatic electron donors at the 2,5,8,11-positions (Figure 2). We varied both the donor–acceptor distance and the electronic properties of the donor to probe the viability of this substitution pattern for use in photoinduced charge-separating systems. *p*-*N,N*-dimethylaminophenyl (pDMA1), *p*-*N,N*-dimethylaminobiphenyl (pDMA2), and *N*-biphenylphenothiazine (PTZ2) donors were chosen because of their favorable oxidation potentials and synthetic accessibility.^{29,30} Furthermore, phenothiazine has additional conjugated rings and a sulfur atom present and thus is expected to be well-suited to stabilize an RP and extend its charge recombination lifetime. We also present the synthesis and characterization of pDMA1 and PTZ2 donors coupled through the imide position of PDI for comparison with the respective headland-substituted PDIs.

RESULTS AND DISCUSSION

Syntheses. The syntheses of compounds 1–4 are detailed in Scheme 1. Headland coupling proceeded through Ru-mediated C–H activation at the headland positions of PDI.²⁵ Arylphenylboronic neopentyl esters are typically used to substitute PDI in these positions because of the optimal balance of high reactivity and low yield of side products. However, several of the investigated donors have poor reactivity under the conditions necessary to generate the precursor boronic acid. The neopentyl ester substituent was used whenever possible; however, certain donors were synthesized using the pinacol ester derivative, which is also reactive in this coupling reaction, although to a lesser extent.^{31,32} The syntheses of the imide-linked donor–acceptor compounds 5 and 6 are shown in Scheme 2. A longer branched

alkyl chain was used in the second imide position to ensure the solubility of these compounds.

Spectroscopy. The steady-state absorption spectra of compounds 1–6 (Figure 3) show the characteristic vibronic progression of PDI with the 0–0 transition centered at 530 nm. The 0–0, 0–1, and 0–2 vibronic bands, at 530, 495, and 460 nm, respectively, are broadened in donor-containing compounds 2–4, with the biphenyl-spaced donors exhibiting less of an effect than the phenyl-spaced donor. Features on the blue edge of the spectra for 2–4 are attributed to donor-group absorption. A broad charge transfer band is present in the spectra of 2 and 3 spanning 550 to 700 nm. Both the broadening of vibronic bands and presence of charge transfer bands in the donor-containing compounds indicate that the donor–PDI electronic interaction is strong at the headland positions. The greatest effect is exhibited when the donor is closest to the PDI core in 2. Extending the distance between the donor and the acceptor in 3 and 4 decreases the electronic coupling and suppresses the spectral distortions as a result. Additionally, the initial Franck–Condon state of 4 is not in the lowest-energy conformation; ground-state phenothiazine has a “bowl”-shaped conformation, while the phenothiazine lowest-excited singlet state and radical cation state are planar.^{33,34} Competition between nuclear reorganization and relaxation back to the ground state diminish the appearance of charge transfer interactions in the ground-state spectrum. Charge transfer interactions are also limited in compounds 5 and 6 because of the presence of a node in the HOMO and LUMO of PDI at the imide position.³⁵

The emission spectrum of 1 shows the expected mirroring of the absorption spectra found in PDI monomers. Unsubstituted PDI typically has a fluorescence quantum yield approaching unity.^{36,37} Thus, the low fluorescence quantum yield of 1 is likely due to partial charge transfer,²⁵ while the complete fluorescence quenching in 2–6 results from complete charge transfer, as determined using femtosecond transient absorption (fsTA) spectroscopy to examine 1–6. The experimental apparatus has been described previously,^{38,39} and the results are summarized in Table 1. Upon photoexcitation at 525 nm, 1 exhibits ground-state bleaching (GSB) from 450 to 560 nm, stimulated emission (SE) from 560 to 600 nm, and a broad excited-state absorption (ESA) from 600 to 850 nm (Figure 4). The GSB, SE, and ESA decay monoexponentially with lifetimes of 753 ± 5 ps in CH_2Cl_2 and 902 ± 3 ps in toluene. These lifetimes are much shorter than the ~ 4 ns lifetime typically reported for ^{1*}PDI; the solvent dependence again indicates that

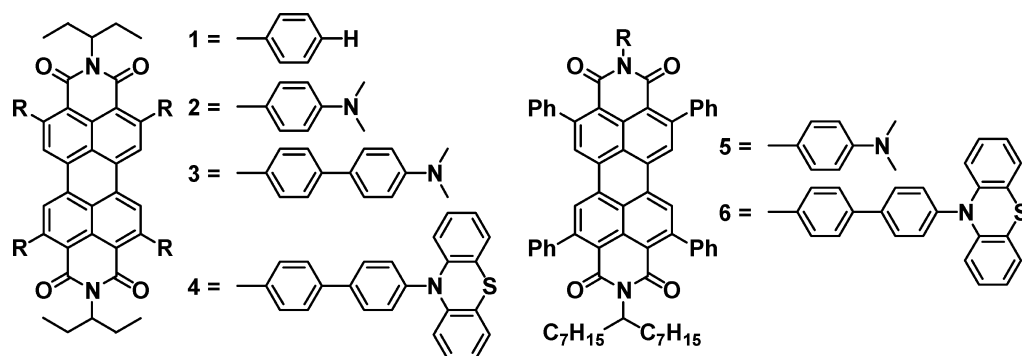
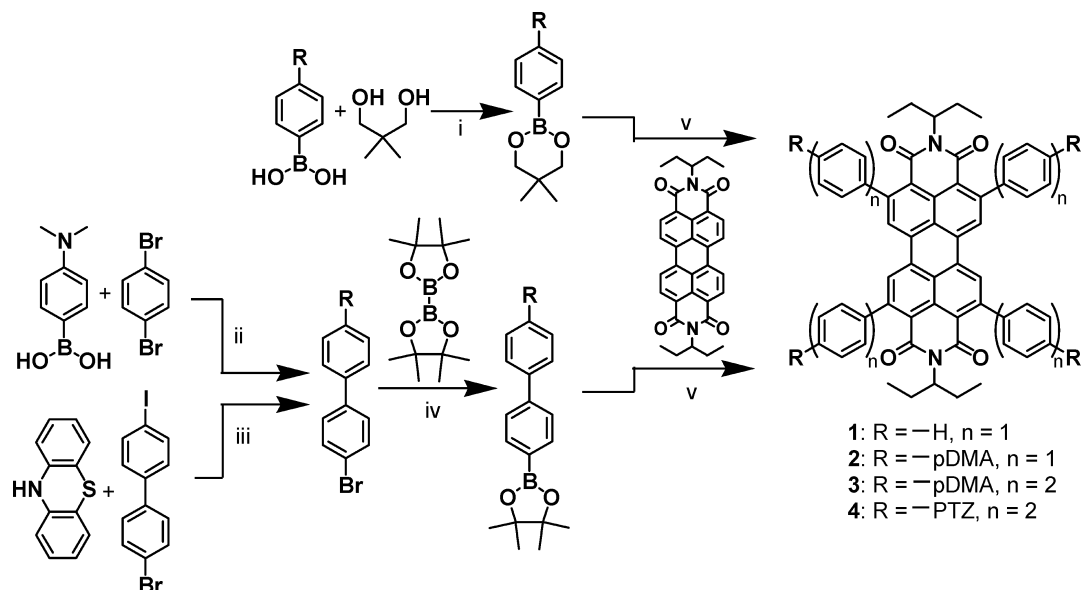
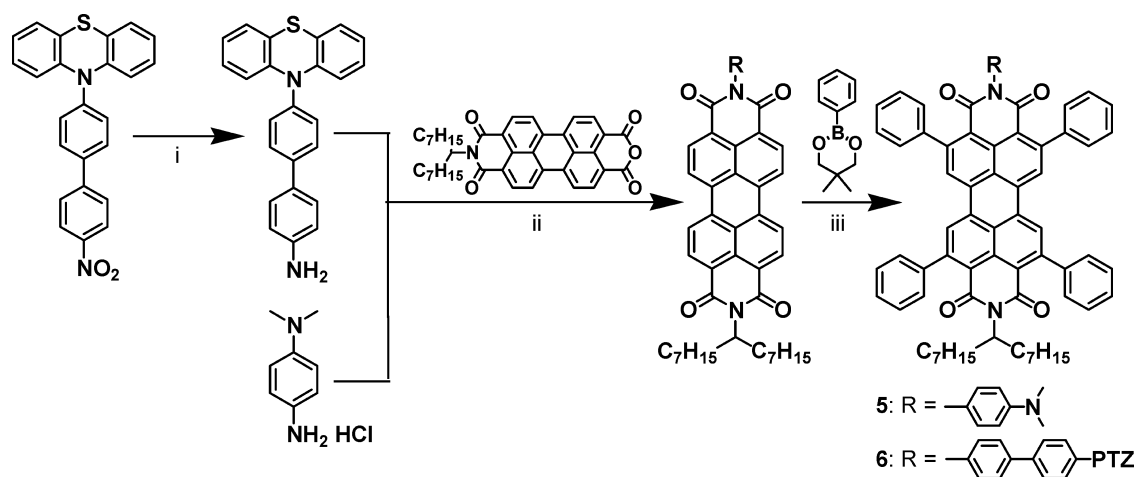


Figure 2. Structures of PDI derivatives 1–6.

Scheme 1. Syntheses of PDI Derivatives 1–4^a

^aReaction conditions: (i) toluene, reflux, 12 h, R = H-, Me₂N-; (ii) Pd(PPh₃)₄, Na₂CO₃, 4:1 THF/H₂O, 80 °C, 12 h; (iii) Pd₂(dba)₃, P(*o*-tol)₃, KO^tBu, toluene, 90 °C, 12 h; (iv) Pd(dppf)Cl₂, KOAc, dioxane, 110 °C, 2 h, R = Me₂N-, phenothiazine-; (v) RuH₂(CO)(PPh₃)₃, 1:1 mesitylene/pinacolone, 140 °C, 72 h.

Scheme 2. Syntheses of PDI Derivatives 5 and 6^a

^aReaction conditions: (i) hydrazine, Pd/C, ethanol, 90 °C, 2 days; (ii) imidazole, pyridine, reflux, 1 day, (iii) RuH₂(CO)(PPh₃)₃, 1:1 mesitylene/pinacolone, 140 °C, 72 h.

charge transfer interactions play a role in the faster relaxation of the excited state.

When a strongly coupled donor is present in the system, as is the case with **2**, the GSB feature persists in the transient spectra, but there is no SE feature, consistent with the completely quenched fluorescence. The absorptive feature, spanning 600–850 nm, also contains a peak at approximately 700 nm, in contrast to the broad, featureless nature of the ESA in **1** (Figure 5). This 700 nm feature decays with lifetimes of 4.7 ± 0.8 ps in CH₂Cl₂ and 26.0 ± 1.0 ps in toluene. As this is a much higher rate than observed for S₁ decay and this system does not exhibit SE, the peak at 700 nm is attributed to PDI^{•-}.⁴⁰ As expected, the solvent polarity impacts the rate of decay of the charged-separated state back to the ground state, with more polar solvents increasing the rate.⁴¹ The PDI^{•-} feature appears within the instrument response function (IRF),

showing that charge separation occurs on a subpicosecond time scale.

The results for **2** verify that charge separation is viable through the headland positions of PDI. However, RP lifetimes longer than 26 ps are needed to make intermolecular charge hopping and/or delocalization within a self-assembled array of donor–acceptor molecules competitive processes.²⁴ One way to extend these charge recombination lifetimes is to decrease the degree of donor–acceptor coupling by extending the distance between them.⁴¹ This decoupling was accomplished in **3** by the addition of a second phenyl spacer group. Once again, PDI^{•-} decay is rapid in CH₂Cl₂ (2.4 ± 0.3 ps) and slower in toluene (58.6 ± 2.0 ps) (Figure 6). Furthermore, the initial charge separation in toluene slows to 2.9 ± 0.7 ps, well beyond the IRF. With this slower initial charge separation, a ~10 nm blue shift is observed, which is attributed to the growth of

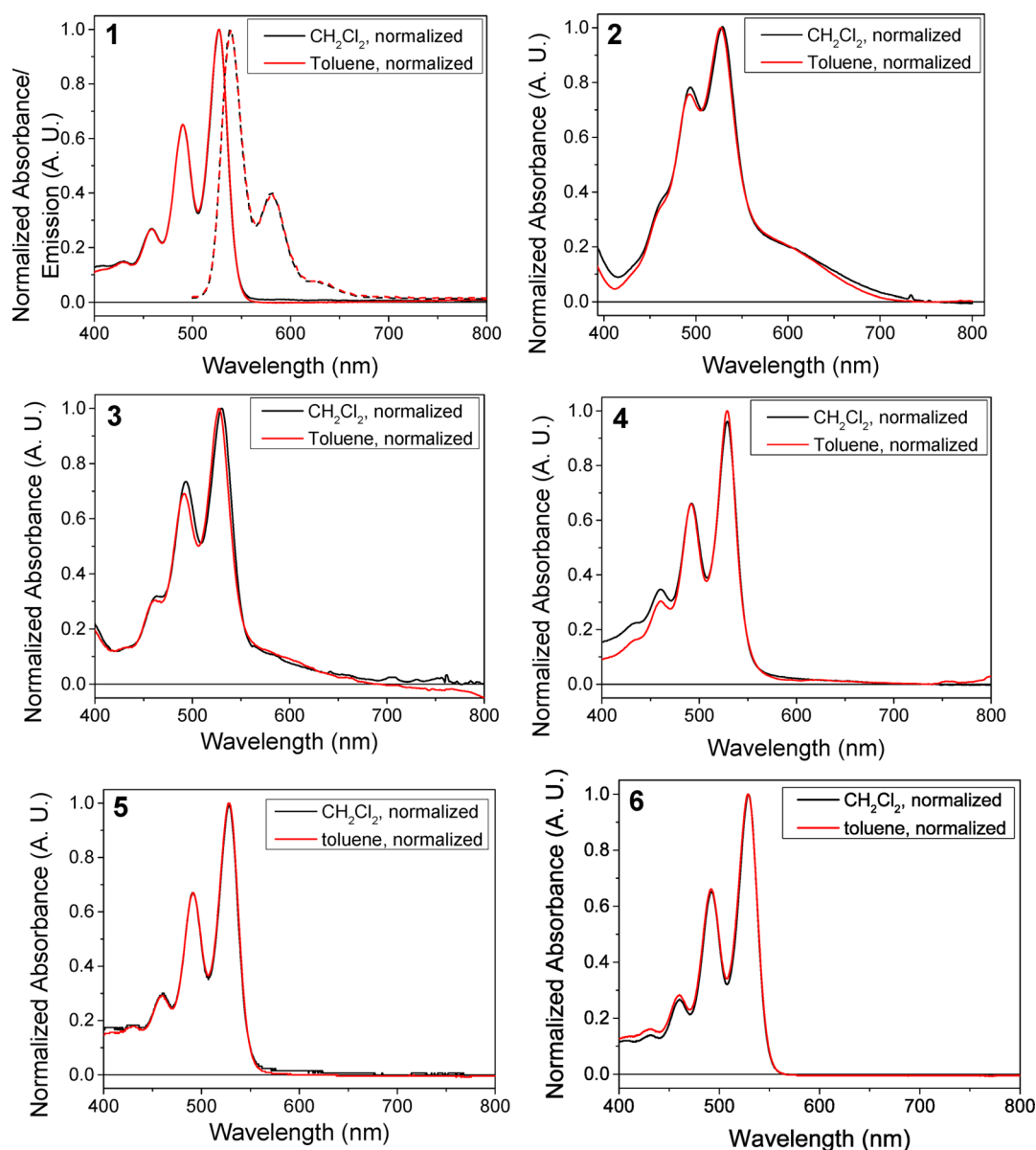


Figure 3. Normalized absorption (solid) and emission (dashed) spectra of 1–6.

Table 1. Summary of fsTA Rates for Compounds 1–6

	CH ₂ Cl ₂		toluene	
	Excited-State Decay (ps)	Excited-State Decay (ps)	Excited-State Decay (ps)	Excited-State Decay (ps)
1	753 ± 5		902 ± 3	
	CS (ps)	CR (ps)	CS (ps)	CR (ps)
2	<1	4.7 ± 0.8	<1	26.0 ± 1.0
3	<1	2.4 ± 0.3	2.9 ± 0.7	58.6 ± 2.0
4	<1	6.7 ± 0.4	3.9 ± 0.3	1930 ± 240
5	<1	2.2 ± 0.1	<1	10.0 ± 1.1
6	33.0 ± 5.8	174 ± 2	20.5 ± 1.9	32700 ± 2100

PDI^{•-}. As further evidence of the slower charge separation, SE is observed in early spectral traces but decays at a rate very similar to the charge separation rate. Although the charge recombination rate in toluene decreases by more than a factor of 2 as a result of the increased the donor–acceptor distance, longer lifetimes are still desired.

While the oxidation potential of PTZ is similar to that of pDMA, its extended conjugation, inclusion of a polarizable

sulfur heteroatom, and large dihedral angle between the phenyl group attached to its nitrogen atom and the phenothiazine core all stabilize the hole generated upon charge separation in 4. As was observed in 3, GSB is present in the spectra of 4 from 450 to 560 nm, with a small SE feature visible from 560 to 600 nm. Once again, charge separation is sufficiently slow in toluene to observe the growth of PDI^{•-} at 600–850 nm (Figure 7) with a time constant of 3.9 ± 0.3 ps. This growth is slightly slower than that observed for 3 but demonstrates that replacement of pDMA donors with PTZ donors has little effect on the charge separation rate. This spectrum decays with time constants of 6.7 ± 0.4 ps in CH₂Cl₂ and 1930 ± 240 ps in toluene; thus, the charge recombination lifetime of 4 is 330 times longer than that of 3, showing that the additional stabilization afforded by the phenothiazine donor has a very large impact on this system. A lifetime approaching 2 ns is a significant improvement toward the regime desired for charge transport. Using a diketopyrrolopyrrole (DPP) electron donor covalently attached to two PDI molecules (PDI-DPP-PDI), we have recently shown that even a

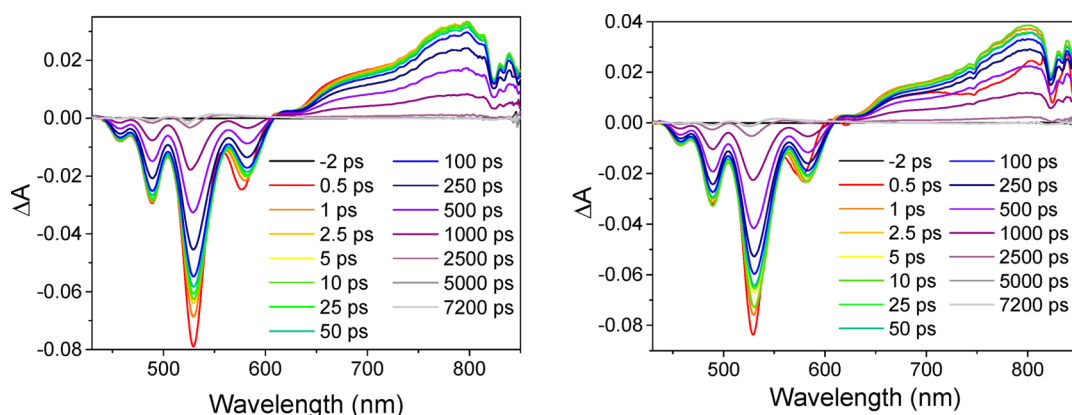


Figure 4. Femtosecond transient absorption spectra of **1** in CH_2Cl_2 (left) and toluene (right).

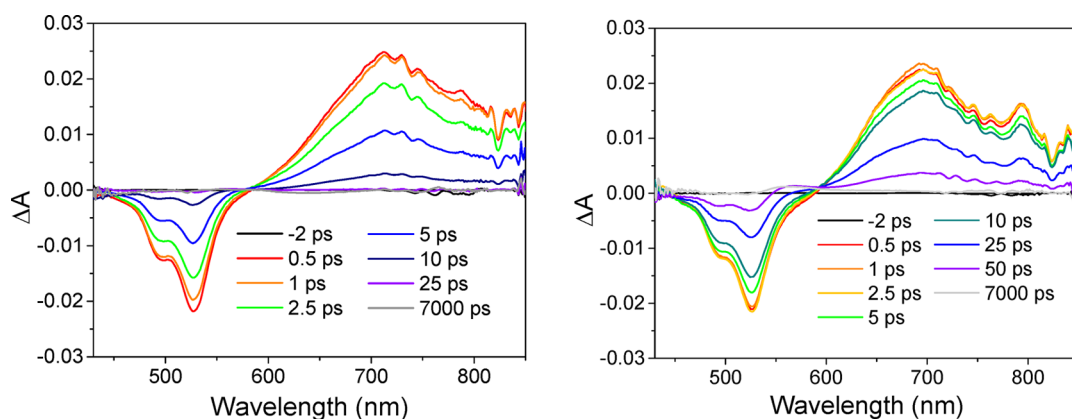


Figure 5. Femtosecond transient absorption spectra of **2** in CH_2Cl_2 (left) and toluene (right).

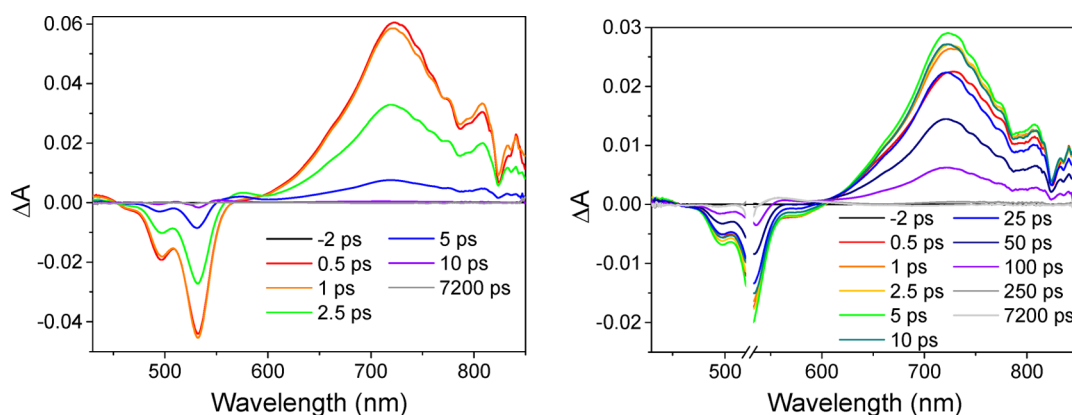


Figure 6. Femtosecond transient absorption spectra of **3** in CH_2Cl_2 (left) and toluene (right).

340 ps charge separation lifetime is sufficient to ensure a 30% yield of free charge carriers in ordered, segregated stacks of solid PDI-DPP-PDI.⁴²

One reason for the much larger difference in RP lifetime of the PTZ donors in toluene versus CH_2Cl_2 relative to that of the pDMA donors may be the significant internal reorganization energy involved in phenothiazine oxidation. In its radical cation state, phenothiazine adopts a flat conformation; while CH_2Cl_2 likely contributes little stabilization to either conformation, the aromatic rings in toluene may better solvate the flat conformation and thus increase the reorganization energy for the charge back-transfer reaction, thus adding another solvent reorganization energy contribution to the overall reorganization

energy. However, the nature of this π – π interaction between toluene and PTZ must be relatively weak because no significant differences in the transient absorption spectra of **4** in CH_2Cl_2 compared to toluene are observed.

An interesting result obtained for **2–4** is the formation of PDI triplet states in low to moderate yields (5–25%) following charge recombination,²⁷ which are visible in the absorptive features at approximately 510 and 550–660 nm. As the headland substituents are oriented at an angle of $\sim 60^\circ$ with respect to the PDI core,^{25,27} intersystem crossing is likely due to a spin–orbit charge transfer (SOCT-ISC) mechanism. This mechanism has been observed previously in systems where the donor and acceptor moieties are offset by a large angle.⁴³ In

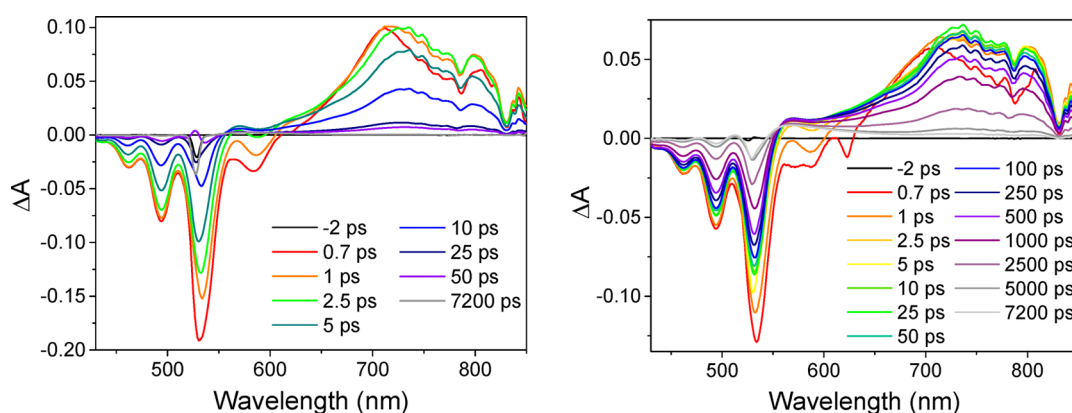


Figure 7. Femtosecond transient absorption spectra of **4** in CH_2Cl_2 (left) and toluene (right).

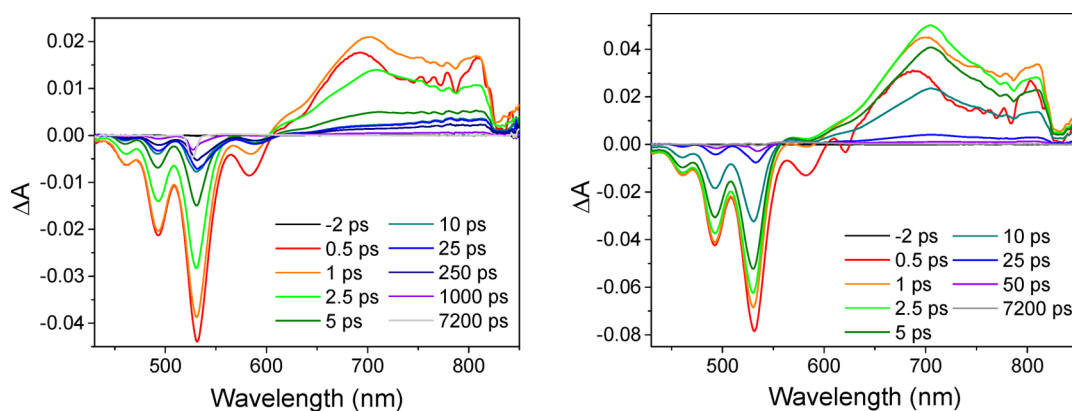


Figure 8. Femtosecond transient absorption spectra of **5** in CH_2Cl_2 (left) and toluene (right).

view of the short RP lifetimes, it is unlikely that triplet formation occurs by the radical-pair intersystem crossing mechanism.^{44–46} Triplet state formation is generally perceived as being detrimental to device efficiency;^{47,48} however, the triplet states in these systems are generated following charge recombination and thus should not be formed competitively in devices, where charge separation is followed by rapid charge extraction.

The donor–acceptor systems **5** and **6** were designed to allow for direct comparison of the electron transfer rates through the headland position with those through the more commonly used imide position. Once again these systems, upon photoexcitation at 525 nm, exhibit GSB from 440 to 560 nm and SE from 560 to 600 nm (Figures 8 and 9, respectively). This SE signal decays rapidly, matching the charge separation dynamics. Charge separation is further verified in toluene by the observation of a red shift and sharpening in the maxima of the absorptive feature from 690 to 705 nm. This charge separation occurs in CH_2Cl_2 with time constants of <1 ps and 33.0 ± 5.8 ps and in toluene with time constants of 2.9 ± 0.7 ps and 20.5 ± 1.9 ps for **5** and **6**, respectively. The relatively large negative free energy for charge separation for **6** may push this reaction into the Marcus inverted regime, as evidenced by the slight decrease in rate in more polar solvents. Recombination to the ground state in these systems again occurs more quickly in CH_2Cl_2 , with lifetimes of 2.2 ± 0.1 ps for **5** and 174 ± 2 ps for **6**. Recombination in toluene occurs in 10.0 ± 1.1 ps and 32.7 ± 2.1 ns for **5** and **6**, respectively.

The clear difference in RP lifetimes for compounds that have the same donor group in different substitution patterns

demonstrates a significant difference in electronic coupling at these positions. While we expect the rates in the imide-substituted compounds to be uniformly lower than the rates in the headland-substituted compounds because of the presence of a node in the HOMO and LUMO at the imide position,⁴⁹ the rate of recombination actually decreases between **2** and **5**. Although the same donor group was used, the connectivity through the imide position significantly impacts the oxidation potential of the pDMA1 donor, shifting it to +1.02 V (Figure S8 in the Supporting Information). Unfortunately, the close proximity of the donor group to the imide group makes **2** an unsuitable model compound, and thus, we cannot use the charge separation or recombination rates to gain reliable information about differences in electronic coupling. However, the addition of a second phenyl spacer group provides greater electronic isolation of the donor from the substituent effect of the imide, and thus, the charge separation and recombination rates for **4** and **6** follow the expected trend. As the electron transfer rate k_{ET} is proportional to V^2 , where V is the electronic coupling matrix element for the reaction,⁵⁰ we can obtain a quantitative measure of the change in electronic coupling by comparing the lifetimes of the processes. In doing so, we determine that the electronic coupling through the headland position is approximately 3.5 times greater than that through the imide position. In cases where competitive rates are a potential issue, as in a multistep charge transfer pathway, the ability to choose between these two electronic coupling regimes can be used to favor the desired process by either increasing or decreasing the charge separation and recombination rates.

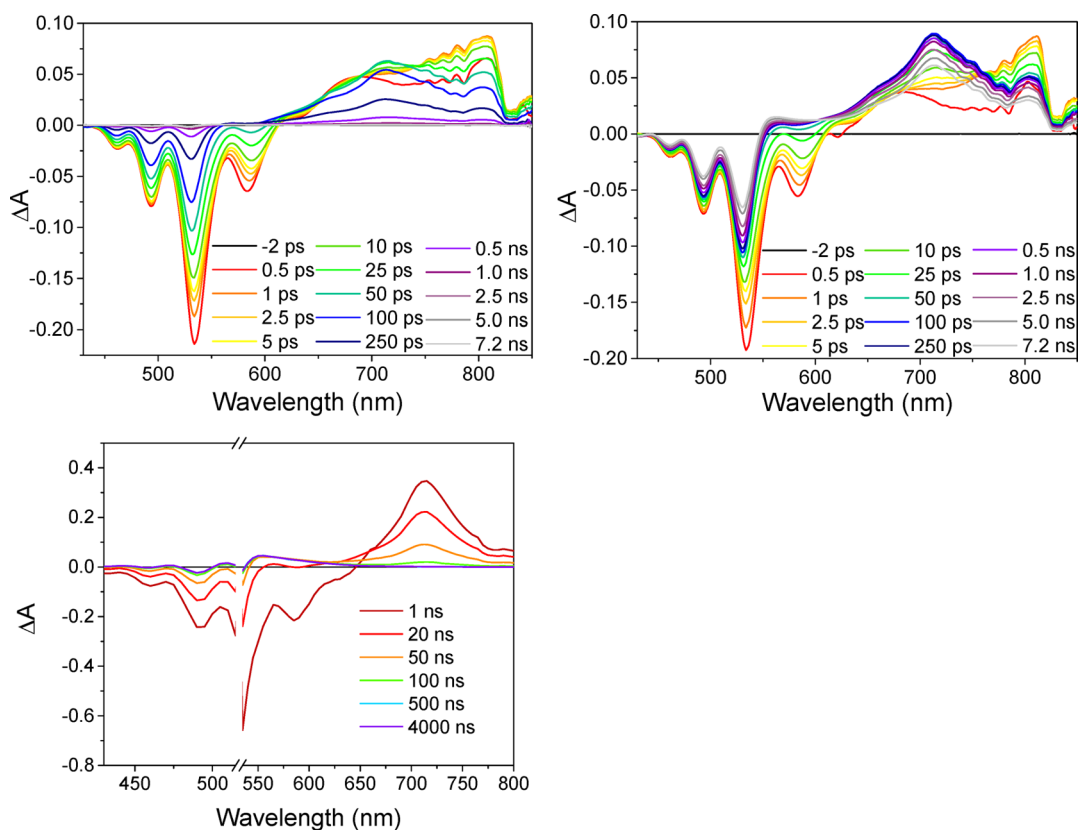


Figure 9. Femtosecond transient absorption spectra of **6** in CH_2Cl_2 (top left) and toluene (top right) and nanosecond transient absorption spectra of **6** in toluene (bottom left).

CONCLUSION

We have presented the synthesis and solution-phase characterization of donor–acceptor systems taking advantage of substitution at the headland positions of PDI. Although the twisting of the intervening phenyl groups between the donor and acceptor may be expected to weaken the electronic coupling,²⁵ the presence of charge transfer bands in the steady-state absorption spectra, the completely quenched fluorescence, and the observation of rapid charge separation in the systems presented here instead imply a much higher degree of electronic interaction. Even the extension of the donor–acceptor distance by addition of another phenyl group decreases this interaction only slightly, slowing the recombination of $\text{PDI}^{\bullet+}$ by a factor of 2. However, providing more stabilization of the radical cation can bring the lifetime of the charge-separated pair into the regime where it begins to be competitive with intermolecular charge transport.

ASSOCIATED CONTENT

Supporting Information

Detailed syntheses and characterization data for **1–6** and additional electrochemical and transient spectroscopy data. This material is available free of charge via the Internet at <http://pubs.acs.org>.

AUTHOR INFORMATION

Corresponding Author

*E-mail: m-wasielewski@northwestern.edu.

Notes

The authors declare no competing financial interest.

ACKNOWLEDGMENTS

This work was supported by the Chemical Sciences, Geosciences, and Biosciences Division, Office of Basic Energy Sciences, U.S. Department of Energy, under Grant DE-FG02-99ER14999.

REFERENCES

- Roncali, J. Single Material Solar Cells: The Next Frontier for Organic Photovoltaics? *Adv. Energy Mater.* **2011**, *1*, 147–160.
- Horowitz, G. Organic Field-Effect Transistors. *Adv. Mater.* **1998**, *10*, 365–377.
- Mishra, A.; Bäuerle, P. Small Molecule Organic Semiconductors on the Move: Promises for Future Solar Energy Technology. *Angew. Chem., Int. Ed.* **2012**, *51*, 2020–2067.
- Sun, Y.; Welch, G. C.; Leong, W. L.; Takacs, C. J.; Bazan, G. C.; Heeger, A. J. Solution-Processed Small-Molecule Solar Cells with 6.7% Efficiency. *Nat. Mater.* **2012**, *11*, 44–48.
- Wang, M.; Wudl, F. Top-Down Meets Bottom-Up: Organized Donor–Acceptor Heterojunctions for Organic Solar Cells. *J. Mater. Chem.* **2012**, *22*, 24297–24314.
- Li, Z.; He, G.; Wan, X.; Liu, Y.; Zhou, J.; Long, G.; Zuo, Y.; Zhang, M.; Chen, Y. Solution Processable Rhodanine-Based Small Molecule Organic Photovoltaic Cells with a Power Conversion Efficiency of 6.1%. *Adv. Energy Mater.* **2012**, *2*, 74–77.
- Walker, B.; Tamayo, A. B.; Dang, X.-D.; Zalar, P.; Seo, J. H.; Garcia, A.; Tantiwivat, M.; Nguyen, T.-Q. Nanoscale Phase Separation and High Photovoltaic Efficiency in Solution-Processed, Small-Molecule Bulk Heterojunction Solar Cells. *Adv. Funct. Mater.* **2009**, *19*, 3063–3069.
- Izawa, S.; Hashimoto, K.; Tajima, K. Morphological Stability of Organic Solar Cells Based Upon an Oligo(P-Phenylenevinylene)-C70 Dyad. *Phys. Chem. Chem. Phys.* **2012**, *14*, 16138–16142.

- (9) Kumar, P.; Shivananda, K. N.; Zajączkowski, W.; Pisula, W.; Eichen, Y.; Tessler, N. The Relation between Molecular Packing or Morphology and Chemical Structure or Processing Conditions: The Effect on Electronic Properties. *Adv. Funct. Mater.* **2014**, *24*, 2530–2536.
- (10) Graham, K. R.; Stalder, R.; Wieruszewski, P. M.; Patel, D. G.; Salazar, D. H.; Reynolds, J. R. Tailor-Made Additives for Morphology Control in Molecular Bulk-Heterojunction Photovoltaics. *ACS Appl. Mater. Interfaces* **2013**, *5*, 63–71.
- (11) Herbst, W.; Hunger, K.; Wilker, G.; Ohleier, H.; Winter, R. In *Industrial Organic Pigments*; Wiley-VCH: Weinheim, Germany, 2005; pp 421–566.
- (12) Langhals, H.; Ismael, R. Cyclophanes as Model Compounds for Permanent, Dynamic Aggregates—Induced Chirality with Strong CD Effects. *Eur. J. Org. Chem.* **1998**, 1915–1917.
- (13) Huang, C.; Barlow, S.; Marder, S. R. Perylene-3,4,9,10-Tetracarboxylic Acid Diimides: Synthesis, Physical Properties, and Use in Organic Electronics. *J. Org. Chem.* **2011**, *76*, 2386–2407.
- (14) Kozma, E.; Catellani, M. Perylene Diimides Based Materials for Organic Solar Cells. *Dyes Pigm.* **2013**, *98*, 160–179.
- (15) Würthner, F.; Thalacker, C.; Sautter, A. Hierarchical Organization of Functional Perylene Chromophores to Mesoscopic Superstructures by Hydrogen Bonding and π - π Interactions. *Adv. Mater.* **1999**, *11*, 754–758.
- (16) Zhang, J.; Hoeben, F. J. M.; Pouderoijen, M. J.; Schenning, A. P. H. J.; Meijer, E. W.; De Schryver, F. C.; De Feyter, S. Hydrogen-Bonded Oligo(*p*-phenylenevinylene) Functionalized with Perylene Bisimide: Self-Assembly and Energy Transfer. *Chem.—Eur. J.* **2006**, *12*, 9046–9055.
- (17) Kaiser, T. E.; Wang, H.; Stepanenko, V.; Würthner, F. Supramolecular Construction of Fluorescent J-Aggregates Based on Hydrogen-Bonded Perylene Dyes. *Angew. Chem., Int. Ed.* **2007**, *46*, 5541–5544.
- (18) Würthner, F.; Kaiser, T. E.; Saha-Möller, C. R. J-Aggregates: From Serendipitous Discovery to Supramolecular Engineering of Functional Dye Materials. *Angew. Chem., Int. Ed.* **2011**, *50*, 3376–3410.
- (19) Würthner, F. Perylene Bisimide Dyes as Versatile Building Blocks for Functional Supramolecular Architectures. *Chem. Commun.* **2004**, 1564–1579.
- (20) Rybtchinski, B.; Sinks, L. E.; Wasielewski, M. R. Photoinduced Electron Transfer in Self-Assembled Dimers of 3-Fold Symmetric Donor–Acceptor Molecules Based on Perylene-3,4,9,10-Bis-(Dicarboximide). *J. Phys. Chem. A* **2004**, *108*, 7497–7505.
- (21) Rybtchinski, B.; Sinks, L. E.; Wasielewski, M. R. Combining Light-Harvesting and Charge Separation in a Self-Assembled Artificial Photosynthetic System Based on Perylenediimide Chromophores. *J. Am. Chem. Soc.* **2004**, *126*, 12268–12269.
- (22) Roznyatovskiy, V. V.; Carmieli, R.; Dyar, S. M.; Brown, K. E.; Wasielewski, M. R. Photodriven Charge Separation and Transport in Self-Assembled Zinc Tetrabenzotetraphenylporphyrin and Perylenediimide Charge Conduits. *Angew. Chem., Int. Ed.* **2014**, *53*, 3457–3461.
- (23) Mickley Conron, S. M.; Shoer, L. E.; Smeigh, A. L.; Ricks, A. B.; Wasielewski, M. R. Photoinitiated Electron Transfer in Zinc Porphyrin–Perylenediimide Cruciforms and Their Self-Assembled Oligomers. *J. Phys. Chem. B* **2013**, *117*, 2195–2204.
- (24) Bullock, J. E.; Carmieli, R.; Mickley, S. M.; Vura-Weis, J.; Wasielewski, M. R. Photoinitiated Charge Transport through π -Stacked Electron Conduits in Supramolecular Ordered Assemblies of Donor–Acceptor Triads. *J. Am. Chem. Soc.* **2009**, *131*, 11919–11929.
- (25) Nakazono, S.; Easwaramoorthi, S.; Kim, D.; Shinokubo, H.; Osuka, A. Synthesis of Arylated Perylene Bisimides through C–H Bond Cleavage under Ruthenium Catalysis. *Org. Lett.* **2009**, *11*, 5426–5429.
- (26) Nakazono, S.; Imazaki, Y.; Yoo, H.; Yang, J.; Sasamori, T.; Tokitoh, N.; Cédric, T.; Kageyama, H.; Kim, D.; Shinokubo, H.; Osuka, A. Regioselective Ru-Catalyzed Direct 2,5,8,11-Alkylation of Perylene Bisimides. *Chem.—Eur. J.* **2009**, *15*, 7530–7533.
- (27) Eaton, S. W.; Shoer, L. E.; Karlen, S. D.; Dyar, S. M.; Margulies, E. A.; Veldkamp, B. S.; Ramanan, C.; Hartzler, D. A.; Savikhin, S.; Marks, T. J.; Wasielewski, M. R. Singlet Exciton Fission in Polycrystalline Thin Films of a Slip-Stacked Perylenediimide. *J. Am. Chem. Soc.* **2013**, *135*, 14701–14712.
- (28) Hartnett, P. E.; Timalsina, A.; Matte, H. S. S. R.; Zhou, N.; Guo, X.; Zhao, W.; Facchetti, A.; Chang, R. P. H.; Hersam, M. C.; Wasielewski, M. R.; Marks, T. J. Slip-Stacked Perylenediimides as an Alternative Strategy for High Efficiency Nonfullerene Acceptors in Organic Photovoltaics. *J. Am. Chem. Soc.* **2014**, *136*, 16345–16356.
- (29) Daub, J.; Engl, R.; Kurzawa, J.; Miller, S. E.; Schneider, S.; Stockmann, A.; Wasielewski, M. R. Competition between Conformational Relaxation and Intramolecular Electron Transfer within Phenothiazine–Pyrene Dyads. *J. Phys. Chem. A* **2001**, *105*, 5655–5665.
- (30) Montalti, M.; Credi, A.; Prodi, L.; Gandolfi, M. T. *Handbook of Photochemistry*, 3rd ed.; CRC Press: Boca Raton, FL, 2006; pp 493–528.
- (31) Kakiuchi, F.; Murai, S. Catalytic C–H/Olefin Coupling. *Acc. Chem. Res.* **2002**, *35*, 826–834.
- (32) Murai, S.; Kakiuchi, F.; Sekine, S.; Tanaka, Y.; Kamatani, A.; Sonoda, M.; Chatani, N. Efficient Catalytic Addition of Aromatic Carbon–Hydrogen Bonds to Olefins. *Nature* **1993**, *366*, 529–531.
- (33) Thériault, K. D.; Sutherland, T. C. Optical and Electrochemical Properties of Ethynylaniline Derivatives of Phenothiazine, Phenothiazine-5-Oxide and Phenothiazine-5,5-Dioxide. *Phys. Chem. Chem. Phys.* **2014**, *16*, 12266–12274.
- (34) Hauck, M.; Stolte, M.; Schönhaber, J.; Kuball, H.-G.; Müller, T. J. J. Synthesis, Electronic, and Electro-optical Properties of Emissive Solvatochromic Phenothiazinyl Merocyanine Dyes. *Chem.—Eur. J.* **2011**, *17*, 9984–9998.
- (35) Lee, S. K.; Zu, Y.; Herrmann, A.; Geerts, Y.; Müllen, K.; Bard, A. J. Electrochemistry, Spectroscopy and Electrogenenerated Chemiluminescence of Perylene, Terrylene, and Quaterylene Diimides in Aprotic Solution. *J. Am. Chem. Soc.* **1999**, *121*, 3513–3520.
- (36) Ford, W. E.; Kamat, P. V. Photochemistry of 3,4,9,10-Perylenetetracarboxylic Dianhydride Dyes. 3. Singlet and Triplet Excited-State Properties of the Bis(2,5-di-*tert*-butylphenyl)imide Derivative. *J. Phys. Chem.* **1987**, *91*, 6373–6380.
- (37) Rademacher, A.; Märkle, S.; Langhals, H. Lösliche Perylen-Fluoreszenzfarbstoffe Mit Hoher Photostabilität. *Chem. Ber.* **1982**, *115*, 2927–2934.
- (38) Bullock, J. E.; Vagnini, M. T.; Ramanan, C.; Co, D. T.; Wilson, T. M.; Dicke, J. W.; Marks, T. J.; Wasielewski, M. R. Photophysics and Redox Properties of Rylene Imide and Diimide Dyes Alkylated Ortho to the Imide Groups. *J. Phys. Chem. B* **2010**, *114*, 1794–1802.
- (39) Kelley, R. F.; Goldsmith, R. H.; Wasielewski, M. R. Ultrafast Energy Transfer within Cyclic Self-Assembled Chlorophyll Tetramers. *J. Am. Chem. Soc.* **2007**, *129*, 6384–6385.
- (40) Gosztola, D.; Niemczyk, M. P.; Svec, W.; Lukas, A. S.; Wasielewski, M. R. Excited Doublet States of Electrochemically Generated Aromatic Imide and Diimide Radical Anions. *J. Phys. Chem. A* **2000**, *104*, 6545–6551.
- (41) Weller, A. Photoinduced Electron Transfer in Solution: Exciplex and Radical Ion Pair Formation Free Enthalpies and Their Solvent Dependence. *Z. Phys. Chem.* **1982**, *133*, 93–98.
- (42) Hartnett, P. E.; Dyar, S. M.; Margulies, E. A.; Shoer, L. E.; Cook, A. W.; Eaton, S. W.; Marks, T. J.; Wasielewski, M. R. Long-Lived Charge Carrier Generation in Ordered Films of a Covalent Perylenediimide–Diketopyrrolopyrrole–Perylenediimide Molecule. *Chem. Sci.* **2014**, DOI: 10.1039/C1034SC02551B.
- (43) Dance, Z. E. X.; Mickley, S. M.; Wilson, T. M.; Ricks, A. B.; Scott, A. M.; Ratner, M. A.; Wasielewski, M. R. Intersystem Crossing Mediated by Photoinduced Intramolecular Charge Transfer: Julolidine–Anthracene Molecules with Perpendicular π Systems. *J. Phys. Chem. A* **2008**, *112*, 4194–4201.
- (44) Closs, G. L.; Forbes, M. D. E.; Norris, J. R. Spin-Polarized Electron-Paramagnetic Resonance-Spectra of Radical Pairs in

Micelles—Observation of Electron Spin–Spin Interactions. *J. Phys. Chem.* **1987**, *91*, 3592–3599.

(45) Buckley, C. D.; Hunter, D. A.; Hore, P. J.; McLauchlan, K. A. Electron Spin Resonance of Spin-Correlated Radical Pairs. *Chem. Phys. Lett.* **1987**, *135*, 307–312.

(46) Hoff, A. J.; Gast, P.; Dzuba, S. A.; Timmel, C. R.; Fursman, C. E.; Hore, P. J. The Nuts and Bolts of Distance Determination and Zero- and Double-Quantum Coherence in Photoinduced Radical Pairs. *Spectrochim. Acta, Part A* **1998**, *54*, 2283–2293.

(47) Rao, A.; Chow, P. C. Y.; Gelinas, S.; Schlenker, C. W.; Li, C.-Z.; Yip, H.-L.; Jen, A. K. Y.; Ginger, D. S.; Friend, R. H. The Role of Spin in the Kinetic Control of Recombination in Organic Photovoltaics. *Nature* **2013**, *500*, 435–439.

(48) Snedden, E. W.; Monkman, A. P.; Dias, F. B. Kinetic Studies of Geminate Polaron Pair Recombination, Dissociation, and Efficient Triplet Exciton Formation in PC:PCBM Organic Photovoltaic Blends. *J. Phys. Chem. C* **2012**, *116*, 4390–4398.

(49) Chaignon, F.; Falkenström, M.; Karlsson, S.; Blart, E.; Odobel, F.; Hammarström, L. Very Large Acceleration of the Photoinduced Electron Transfer in a Ru(Bpy)₃–Naphthalene Bisimide Dyad Bridged on the Naphthyl Core. *Chem. Commun.* **2007**, 64–66.

(50) Bixon, M.; Jortner, J.; Verhoeven, J. W. Lifetimes for Radiative Charge Recombination in Donor–Acceptor Molecules. *J. Am. Chem. Soc.* **1994**, *116*, 7349–7355.